Single-crystal neutron-diffraction study of the orientational glass state of $(NaCN)_{1-x}(KCN)_x$

T. Schräder and A. Loidl
Institut für Physik, Universität Mainz, D-6500 Mainz, Federal Republic of Germany

G. J. McIntyre and C. M. E. Zeyen
Institut Laue-Langevin, Boîte Postale 156X, F-38042 Grenoble CEDEX, France
(Received 27 February 1990)

Single crystals of $(NaCN)_{1-x}(KCN)_x$ with concentrations $x=0.19$, 0.44, and 0.89 have been investigated by elastic neutron diffraction. The mixed crystals with $x=0.19$ and 0.44 exhibit a transition to an orientational glass state, while those with $x=0.89$ transform into a coexistence region of cubic and rhombohedral phases. Diffuse scattered intensities have been studied as a function of temperature T, phonon wave vector $\mathbf{q}$, and momentum transfer $\mathbf{Q}$. $I(T,\mathbf{q},\mathbf{Q})$ provides insight into the character of the freezing process. From a detailed analysis of the structure factors, the orientational distribution of the CN molecules was determined. With increasing strength of random fields, $\langle 100\rangle$ orientations are favored.

I. INTRODUCTION

Disorder phenomena embody a broad field of growing interest in solid-state physics. The dynamic and static behavior of model systems is intensively studied to elucidate the physics of disordered materials. Orientational glasses are crystalline solids which consist of a regular lattice with some sites occupied partly by single atoms and partly by molecules with multipolar moments. These mixed crystals are close to an instability where the moments exhibit orientational order. Below some critical concentration x_c the orientational degrees of freedom freeze-in devoid of long-range order. Prominent examples are alkali-cyanide–alkali-halide solid solutions and mixtures of alkali cyanides.[1-3] In cyanide glasses the freezing-in of orientational disorder leads, via a strong rotation-translation coupling, to frozen-in lattice strains. Single-crystal diffraction experiments have revealed that the onset of freezing is accompanied by a growth of anisotropic patterns of diffuse scattering intensities which appear around the Bragg reflections.[4-9] In inelastic-neutron-scattering experiments these intensities appear as an additional central component and can be related to the "glass order parameter."[4,5]

In the early work of Michel and Rowe,[5] the diffuse intensities have been explained starting from a microscopic lattice-dynamical description. Within the approximations used in that work, the dependence of the diffuse intensities on the phonon wave vector $\mathbf{q}$ is given by $I(q)=A/q+B/q^2$, with $\mathbf{q}\equiv(\xi_1,\xi_2,\xi_3)=\mathbf{Q}-\tau_{hkl}$. Here, $\mathbf{Q}$ is the total momentum transfer and τ_{hkl} indicates a reciprocal-lattice vector. The linear term accounts for the observed asymmetry in $(KBr)_{1-x}(KCN)_x$.[4-6,8] From symmetry arguments $(h00)$-type reflections display only symmetric contributions. At concentrations well below the critical concentration x_c, detailed single-crystal diffraction experiments have been performed by Wochner *et al.*[10,11] Their results were satisfactorily explained within the framework of Huang diffuse scattering, and the observed neutron intensities could be described by $I(q)=A/q+B/q^2$. However, results by Knorr and Loidl[7] and by Loidl *et al.*[6,8,9] on the mixed cyanides $(KCl)_{1-x}(KCN)_x$ and $(KBr)_{1-x}(KCN)_x$ close to x_c showed the failure of the approximations made in this theory. The observation of exponential line shapes and a strong dependence of the exponent on the reciprocal-lattice vector τ_{hkl} were interpreted as a loss of long-range translational order.

Mayer and Cowley[12] calculated the neutron-scattering cross section of crystals assuming a second-order planar ferroelastic instability without making the usual phonon expansion in a power series in small displacements. They found that at T_c, long-range translational order is destroyed and the scattering function at the reciprocal-lattice points is described by power laws. Subsequently, Mayer and Cowley[13] investigated the effect of random stresses in these systems and found that these drive the transition to first order. This latter observation is in conflict with the experimental evidence in $(KBr)_{1-x}(KCN)_x$ and $(NaCN)_{1-x}(KCN)_x$, where random-strain fields appear to drive the first-order phase transition of the pure compounds almost to second order near x_c.[7,14]

A random-strain model was proposed by Michel[15] for orientational glasses. Within this model the x-T phase diagrams and quadrupolar susceptibilities were calculated for the cyanide glasses. The "glass order parameter" was found to vary smoothly as a function of temperature, following $1/T^2$ at high temperatures. Later, Michel and Bostoen extended this theory including a nonergodic instability.[16] At T_{NE} an abrupt increase of diffuse scattering was predicted and the q and T dependences of the diffuse intensities were calculated in detail (NE denotes nonergodic).

$(NaCN)_{1-x}(KCN)_x$ mixed crystals show an orientational glass state for an intermediate range of composition $0.16=x_{c1}\lesssim x\lesssim x_{c2}=0.9$.[14,17-19] It was proposed[15] that the low-temperature states of these mixed crystals

are determined by competing interactions: the translation-rotation coupling (TRC) drives cooperative phenomena of orientations which lead to structural phase transitions and long-range orientational order at low temperatures. The random strain-rotation coupling (RSRC) promotes single-particle behavior and freezing into random orientations. In a first approximation the strength of the TRC should scale linearly with the concentration x between the pure systems NaCN and KCN, while the strength of the RSRC varies as $x(1-x)$.[14,17–19] Thus the competition between the interactions can be tuned by varying the concentration x.

The aim of this work was to study the temperature and Q dependences of the diffuse scattered intensities in the glassy region of $(NaCN)_{1-x}(KCN)_x$. Of special interest was the concentration-dependent interplay of RSRC and TRC and how this competition shows up in the diffuse scattering intensities.

II. EXPERIMENT

Single crystals with concentrations of $x=0.19$, 0.44, and 0.89 were supplied by J. Albers of the Universität des Saarlandes, Saarbrücken, FRG. They were grown from the melt by a conventional Czochralski technique. The x values given in this work denote the K^+ concentration of the mixed crystals as determined from the room-temperature lattice constants.[19] The samples used in this study were cleaved from the same boules as those crystals used for ultrasonic,[20] inelastic-neutron-scattering,[20] and powder-diffraction experiments.[14,19] The neutron-diffraction experiments were carried out on the four-circle spectrometer D10 located on a thermal-neutron guide at the Institut Laue-Langevin, Grenoble. Samples of approximately $5\times5\times8$ mm^3 were cut from larger single crystals and were mounted on an Eulerian cradle, which allows scans along all reciprocal-lattice directions. A vertical focusing Cu(200) monochromator selected neutrons with a wavelength of 1.26 Å. To define the energy resolution and to lower the background, a pyrolytic graphite (004) analyzer was used set to zero energy transfer with an energy resolution of approximately 1.5 meV.

The Q resolution convoluted with the mosiac spread of the samples gave a typical transverse width of $\Delta Q_y - 0.008(2\pi/a)$ for the (200) reflections. The width of longitudinal scans through (200) reflections was about $\Delta Q_x = 0.04(2\pi/a)$. A He-flow cyrostat which provides full four-circle accessibility[21] allowed a variation of temperature from 300 to 9 K with an accuracy of better than 0.1 K.

III. RESULTS AND ANALYSIS

A. Diffraction profiles

1. $(NaCN)_{0.81}(KCN)_{0.19}$

Crystals with a concentration of $x=0.19$ have been studied previously by inelastic-neutron-scattering and ultrasonic experiments.[20] The intensity of the critical component, as observed in energy scans of inelastic-neutron experiments, was found to be a smooth function of temperature. At high temperatures the central peak intensity followed roughly a $1/T^2$ behavior, in accordance with the predictions of the pure random-strain model.[15]

Figure 1 displays typical spectra of transverse elastic scans along the [010] direction through the (600) reciprocal-lattice point measured at different temperatures. Upon cooling, in addition to the Bragg peak, an increasing diffuse contribution becomes apparent. The pure Bragg component was fitted using a Gaussian line shape. With decreasing temperatures the intensity of the Bragg peak increases slightly, to pass through a maximum at 100 K, and then decreases. We note that at room temperature the width of the elastic line is determined by the resolution of the spectrometer, but increases slightly below 150 K. The appearance of diffuse scattered intensity is a well-documented phenomenon in the cyanide glasses[4,6,8,9] and has been suggested to result from frozen-in shear strains. The line shapes of the diffuse component have been reported to be exponential.[6–9] In this work Lorentzian as well as exponential line shapes were used to fit the diffuse components of $x=0.19$. However, the χ^2 values indicated an insignificant difference in the quality of fits for these different line shapes. Therefore the diffuse contributions

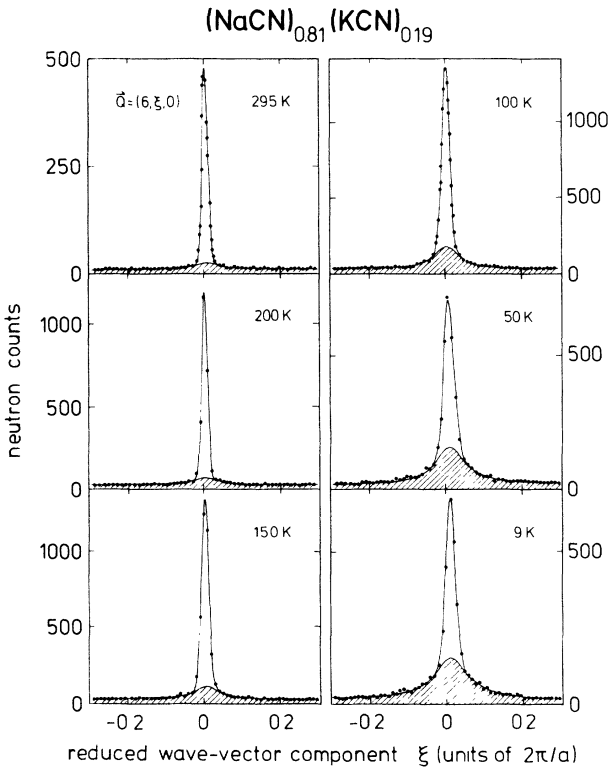

FIG. 1. Transverse scans along [010] at zero energy transfer through the (600) reflection of $(NaCN)_{0.81}(KCN)_{0.19}$ at various temperatures. The hatched areas show the contribution from shear strains and the unhatched areas that from Bragg scattering. The solid lines represent fits to the observed data as explained in the text.

were arbitrarily fitted by Lorentzian functions as represented in Fig. 1 by solid lines. Longitudinal scans along the [100] direction show no diffuse intensities and confirm that the diffuse scattered contributions originate from shear distortions of T_{2g} symmetry.[4-9]

In Fig. 2 the integrated intensities of the Gaussian component A_G, the Lorentzian component A_L, and the total peak area are plotted versus T. Upon cooling, the diffuse intensities A_L continuously increase and saturate below 80 K. At the same time, $A_G(T)$ increases less weakly than expected for a usual harmonic crystal and passes through a maximum near $T=120$ K. The ratio of the Gaussian to Lorentzian component, A_G/A_L, changes from 80% at room temperature to 41% at 9 K. The total intensity displays a maximum at 80 K. This behavior reveals an anomalous Debye-Waller factor, which can be viewed as purely static at low temperatures. It should be noted that the width of the Lorentzian line slightly increases for $T < 150$ K.

The investigations of $(KBr)_{0.50}(KCN)_{0.50}$ (Refs. 4 and 5) showed that at the glass-transition temperature the diffuse components start to grow, and can be described in terms of a nonzero order parameter only below T_s. However, in $(NaCN)_{0.81}(KCN)_{0.19}$, $A_L(T)$ is nonzero at room temperature and does not exhibit any discontinuity at temperatures corresponding to the minimum of $c_{44}(T)$.[20] At THz frequencies the minimum in $c_{44}(T)$ appears at $T\approx 150$ K. Since the central component observed in inelastic-neutron-scattering experiments results from the diffuse pattern around the cubic Bragg positions, "order-parameter behavior" should also be expected for $A_L(T)$. Here the term "order parameter" is used in accordance with the nomenclature in literature.[15,16] However, a conventional order parameter implies a characteristic glass-transition temperature. In Fig. 2 the dashed line represents the theoretically predicted power law $\psi\sim 1/T^2$. The high-T behavior of $A_L(T)$ is in rough agreement with the predictions of Michel's theory[15] and confirms the earlier inelastic-neutron-scattering experiments. Saturation effects set in at low temperatures.

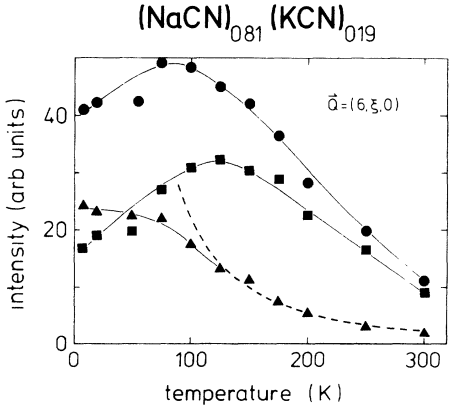

FIG. 2. Temperature dependence of the Bragg intensities [Gaussian area (A_g): ■] of the quasielastic contributions [Lorentzian areas (A_L): ▲] and of the total peak area (●) as measured in the (001) plane at the (600) reciprocal lattice point in $(NaCN)_{0.81}(KCN)_{0.19}$. Solid lines are drawn to guide the eye; the dashed line represents a $1/T^2$ power law.

2. $(NaCN)_{0.56}(KCN)_{0.44}$

For the mixed crystal with $x=0.44$ strong random strain-rotation coupling is expected. Figure 3 displays elastic scans along the [010] direction through the reciprocal-lattice points (220) and (440) for the high-T plastic phase at 295 K and for the low-T state at 10 K. For all reflections investigated, the temperature-dependent anisotropic broadening is almost negligible. This is true for the symmetric contributions of the ($0h0$) reflections and for the symmetric and asymmetric contributions of the ($hh0$) reflections. The spectra are quite similar at all temperatures and are dominated by pure Bragg scattering.

In Fig. 4 the temperature dependences of A_G, A_L, and the total integrated peak intensities are plotted as determined from fits to transverse scans along [010] through the (600) reflection. The diffuse component increases only slightly for decreasing temperature. However, the nonzero diffuse component at low T indicates that the crystal is definitely not free of strains, but even the spectra at 10 K indicate only a minor disturbance of the high-T cubic symmetry. From this observation we could speculate that an almost single-ion freezing process takes place in crystals with strong random fields. Thus the cubic symmetry is also preserved in crystals with an undiluted CN sublattice. $A_L(T)$ varies more weakly than $1/T^2$, as indicated by the dashed line in Fig. 4. A similar behavior has been observed for $x=0.59$ by inelastic neutron scattering,[20] which displays only a weak softening of $c_{44}(T)$ and a concomitant slight increase of the central

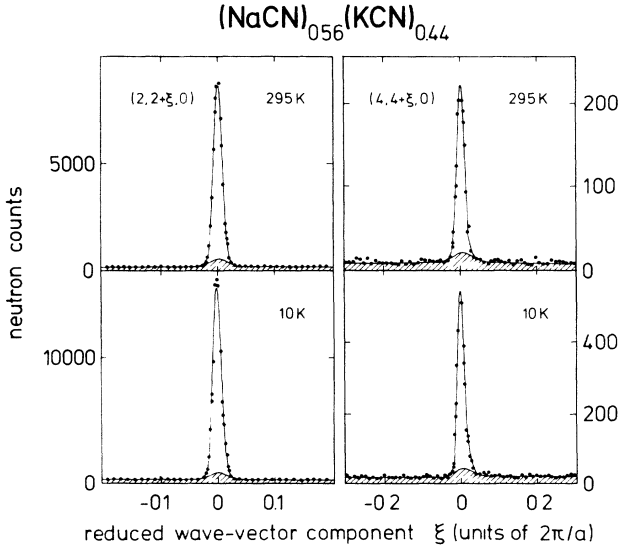

FIG. 3. [010] scans through reciprocal-lattice points of type ($hh0$) in $(NaCN)_{0.56}(KCN)_{0.44}$ at room temperature and at 10 K. The hatched areas show the contributions from shear strains and the unhatched areas that from Bragg scattering. Solid lines represent fits to the observed data, as explained in the text.

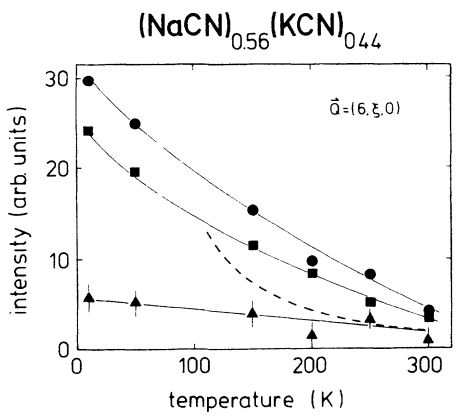

FIG. 4. Temperature dependence of the Bragg intensities (Gaussian area A_G: ■) of the quasielastic contribution (Lorentzian area A_L: ▲) and of the total peak area (●) as measured in the (001) plane at the (600) reciprocal-lattice point of $(NaCN)_{0.56}(KCN)_{0.44}$. Solid lines are drawn to guide the eye; the dashed line shows a $1/T^2$ dependence.

peak intensities for decreasing temperatures. The T dependence of the central component was described by a power law $\psi \sim T^{-m}$, with an exponent $m \approx 0.5$, far below what was expected for a crystal with pure random strain.[15,16] Obviously, at intermediate concentrations $(NaCN)_{1-x}(KCN)_x$ is dominated by strong random fields h, and the high-T limit $h^2/T^2 \ll 1$ fails. Hence it seems essential that in the expansion of the orientation-strain coupling higher-order terms should be taken into account.

3. $(NaCN)_{0.11}(KCN)_{0.89}$

The mixed crystal with $x=0.89$ is almost close to the critical concentration $x_{c2}=0.90$. $(NaCN)_{0.11}(KCN)_{0.89}$ undergoes a phase transformation into a coexistence region of the cubic and rhombohedral structures at $T \approx 100$ K. Figure 5 presents the temperature dependence of transverse elastic scans in the (001) plane through the (600) reciprocal-lattice point. At room temperature the well-defined Gaussian Bragg peak is accompanied by a small amount of diffuse scattered intensity with a Lorentzian distribution. For decreasing temperature the Gaussian component decreases and finally vanishes near 100 K. The profile at 100 K is dominated by the diffuse scattered intensity and can be described by a single Lorentzian.

The peak areas of the diffuse contribution A_L and of the Gaussian component A_G were calculated from the fits to the experimental data. $A_L(T)$, $A_G(T)$, and the total integrated peak intensities $A_t(T)$ are depicted in Fig. 6. A comparison with Fig. 2 reveals that the behavior is completely different from the findings for $x=0.19$. The temperature dependence of the total area exhibits a maximum near 200 K and a strong decrease upon further cooling. Below 100 K the total intensity of the cubic (600) reflection is reduced through the transition into a

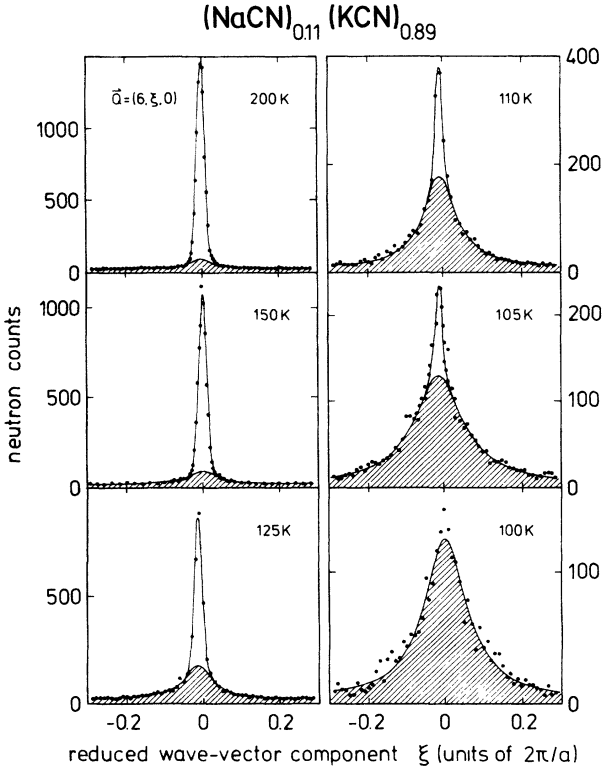

FIG. 5. Transverse scans along [010] at zero energy transfer through the (600) reflection of $(NaCN)_{0.11}(KCN)_{0.89}$ at various temperatures. The hatched areas show the contribution from shear strains and the unhatched areas that from Bragg scattering. Solid lines represent fits to the observed data, as explained in the text.

coexistence region of cubic and rhombohedral phases. $A_G(T)$ also increases down to 200 K. Below 200 K a strong decrease is apparent and the Gaussian component of the (600) reflection vanishes completely near the transition temperature. $A_L(T)$ shows a continuous increase

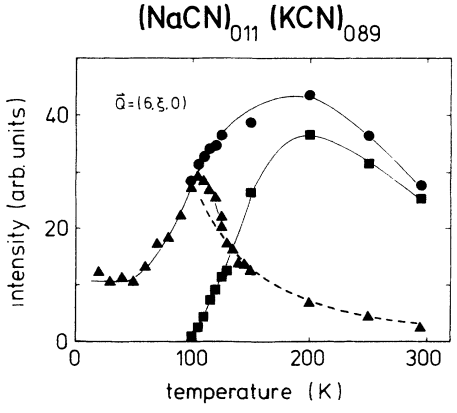

FIG. 6. Temperature dependence of the Bragg intensities (Gaussian area A_G: ■) of the quasielastic contribution (Lorentzian area A_L: ▲) and of the total peak area (●) as measured in the (001) plane at the (600) reciprocal-lattice point in $(NaCN)_{0.11}(KCN)_{0.89}$. Solid lines are drawn to guide the eye; the dashed line represents a $1/T^2$ power law.

upon cooling and a sharp maximum near 100 K. Below this temperature the diffuse intensities are reduced by the structural transition. In Fig. 6 the theoretically predicted $1/T^2$ behavior is represented by the dashed line. For high temperatures $A_L(T)$ is in reasonable agreement with the model predictions.[15] Small but significant extra contributions became apparent below 120 K.

For $T=105$ K, just above the transition temperature, we studied the **Q** dependence of the diffuse scattered contributions in more detail. Transverse scans in the [010] direction (q_y scans) were performed for various reciprocal-lattice points of type ($h00$) and ($hh0$). The results are shown in Fig. 7. Gaussian components are only visible for $h^2+k^2+l^2 \lesssim 36$. The (800) reflection definitely can be described by a pure Lorentzian line shape only. The strong decrease of the Gaussian component with increasing momentum transfer **Q** implies an unusually large Debye-Waller factor at 150 K.

The [010] scans through reflections of type ($hh0$) display an asymmetric pattern. The profile at the (220) reciprocal-lattice point is dominated by a strong Gaussian contribution. However, the q_y scan through the (440) reflection shows an extremely asymmetric line shape. Michel and Rowe[5] theoretically described the diffuse intensities by a symmetric term with a Q^2/q^2 dependence and an additional antisymmetric term with a Q/q dependence. Figure 8 shows the ratio of the symmetric to the antisymmetric contribution as determined for the (220) and (440) reflections. For the (220) line the symmetric part dominates the diffuse contribution, and the overall asymmetry of the diffuse component is weak. At higher momentum transfer **Q**, the antisymmetric term becomes stronger and results in an unusual line shape for the (440) line. For the (440) reflection the asymmetric width exceeds the symmetric width, which results in a local minimum of the intensity near the (4,3.9,0) Bragg position.

The Lorenztian line shapes and the strong dependence of the diffuse intensities on the total momentum transfer **Q** are in clear disagreement with the theoretical predictions for Huang scattering. Figure 9 shows the intensity profiles of $(h,\xi,0)$ scans at reciprocal-lattice points with $h=2,4,6,8$ for $x=0.89$ at $T=105$ K. For ease of comparison with the theoretical predictions of Mayer *et al.*[12] and the experimental results of Loidl *et al.*,[8] they are plotted on a semilogarithmic scale. As demonstrated by the linear dependence in this plot, the profile can also be well described by an exponential decay $I_{h00}=I^0_{h00}\exp(\lambda_{h00}\xi)$. Deviations between Lorentzian and exponential descriptions, appear only for small and high values of the reduced wave-vector component ξ, yielding comparable χ^2 values for fits to the measured profiles. The inset of Fig. 9 shows the **Q** dependence of the full width at half maximum (FWHM) of the diffuse scattered contribution as determined from the decay constant λ.

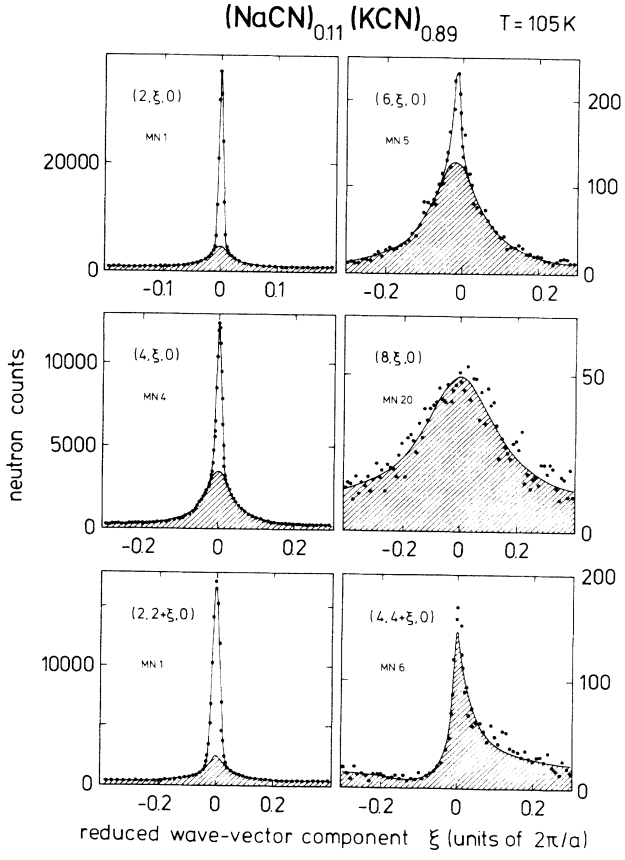

FIG. 7. [010] scans through reciprocal-lattice points of the type ($h00$) and ($hh0$) in $(NaCN)_{0.11}(KCN)_{0.89}$ at 105 K. The hatched areas show the contributions from shear strains and the unhatched areas that from Bragg scattering. Solid lines represent fits to the observed data as explained in the text. Note that the spectra are measured with different monitor rates. The monitor rate is indicated by MN.

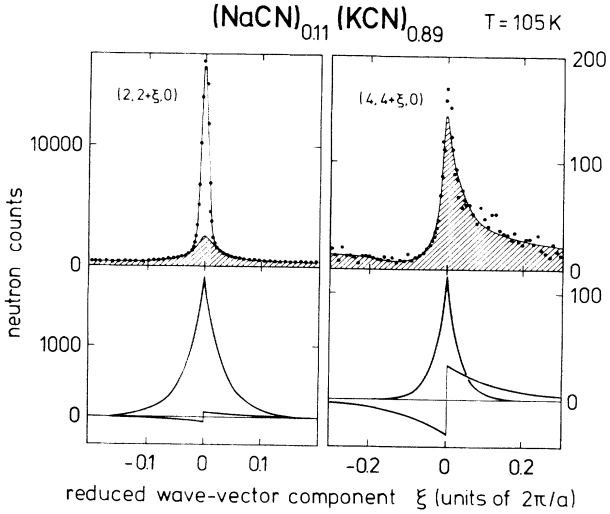

FIG. 8. [010] scans in the (001) plane through the (2,2,0) and (440) reciprocal-lattice points of $(NaCN)_{0.11}(KCN)_{0.89}$. In the upper panels the hatched areas give the total diffuse intensity as determined by fits to the data points. The lower panels show the deconvolution of the diffuse scattered intensities into symmetric and antisymmetric contributions. Note the different intensity scales for the upper and lower panels.

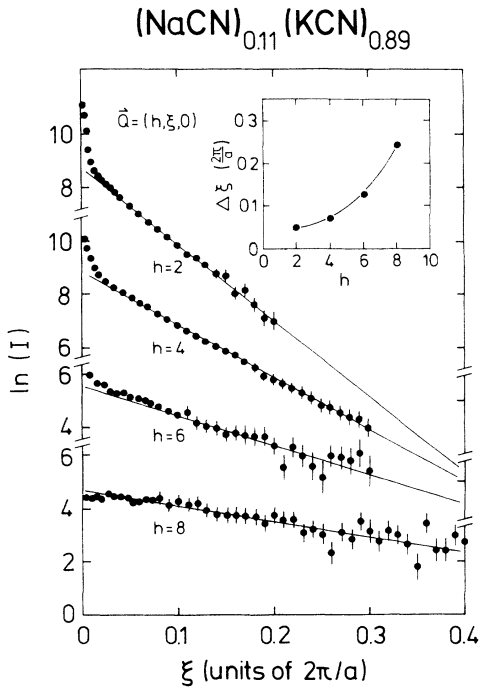

FIG. 9. Intensity profiles for transverse scans through (h00) reflections with $h=2$, 4, 6, and 8 shown on a logarithmic scale. Assuming exponential line shapes, the FWHM's of the diffuse contributions are determined from the slope of the linear part of $\ln[I(\xi)]$ and are shown in the inset.

The strong Q dependence of the "line broadening" is not consistent with an interpretation of the observed diffuse intensities in terms of Huang diffuse scattering.[10,11] It has been shown by Mayer and Cowley[12] that in crystals with a continuous two-dimensional elastic instability long-range order is destroyed at T_c. These authors calculated the scattering cross section and found that close to the phase transition the Bragg peaks disappear and are replaced by power-law singularities. Specifically, they derived the result that the exponents depend significantly on Q. $(NaCN)_{0.11}(KCN)_{0.89}$ shows a planar shear instability near $T_c \approx 100$ K which is close to second order. The observed Q dependence of the diffuse scattering is in qualitative agreement with the predictions of Mayer and Cowley;[12] however, the proposed power-law behavior of $I_{\text{diff}}(\xi)$ could not be confirmed by this experiment. Nevertheless, it may be a useful picture that in the glass regime of mixed cyanides close to x_c, a quasi-two-dimensional fluid phase is frozen-in at low temperatures. The question arises whether there is a close connection between the Mayer-Cowley melting transition[12] and the nonergodic instability proposed by Michel.[16]

B. Orientational distribution

At room temperature the orientational distribution of the CN^- molecules in $(NaCN)_{1-x}(KCN)_x$ was determined from a detailed analysis of the measured structure factors F_{hkl}. A number of 34 independent Bragg reflections was recorded. For each F_{hkl} the intensities of three equivalent reflections were averaged. To explain the Q dependence of the measured structure factor, we applied a model of a preferred orientational distribution of CN^- molecules.[22,23] The orientational probability distribution has been expanded in linear combinations of spherical harmonics adapted to cubic symmetry.[24] Only the first three cubic harmonics with $l=0$, 4, and 6 were used. Parameters of the model are the expansion coefficients γ_4, γ_6, ($\gamma_0=1$), the bond length l of the CN^- molecule, isotropic mean-square displacements $\langle u_\alpha^2 \rangle$ for the alkali-metal ions, and isotropic mean-square displacements for the CN^- ions. Fits with anisotropic mean-square displacements increased the number of parameters, but did not increase the significance of the fits. Typical values for the weighted R factors were $R_w \approx 4.5\%$, with $R_w = \{\sum_i [w_i(I_{i\,\text{obs}} - I_{i\,\text{calc}})]^2 / \sum_i w_i (I_{i\,\text{obs}})^2\}^{1/2}$; $w_i = 1/I_{i\,\text{obs}}$.

The concentration dependence of the mean-square displacements as determined from the best fits to the observed structure factor at 295 K is illustrated in Fig. 10(a). The values for the pure cyanides with $x=0$ and 1 are from Refs. 23 and 8. The values determined for the metal ions and for the CN^- molecules are of comparable magnitude. Deviations are only apparent for pure NaCN. For increasing cationic disorder the vibrational amplitudes decrease towards a slightly minimum at $x=0.5$.

In Fig. 10(b) the expansion coefficients γ_4 and γ_6 which describe the orientational distribution of the CN^- molecules at 295 K are plotted versus the concentration. For the mixed crystals investigated both parameters drastically deviate from a linear interpolation between the values determined for the pure cyanides.[8,23] Despite the large

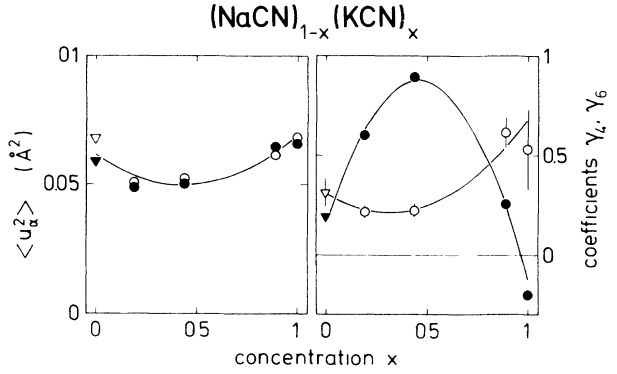

FIG. 10. (a) Concentration dependence of isotropic mean-square displacements in $(NaCN)_{1-x}(KCN)_x$ as determined at room temperature. Values for the center-of-mass motion of the CN^- molecules are shown by solid symbols and values for the metal ions are represented by open symbols. The data for $x=0$ and 1 were taken from Refs. 23 and 8. (b) Concentration dependence of the coefficients γ_4 and γ_6, determined for $(NaCN)_{1-x}(KCN)_x$ at 295 K. γ_4 is represented by solid and γ_6 by open symbols. Data for $x=0$ and 1 were taken from Refs. 23 and 8. Note that $\gamma_4(x)$ changes sign close to $x=1$. The solid lines represent fits to the data assuming an x dependence of $x(1-x)$, superimposed on a linear background of nonzero slope.

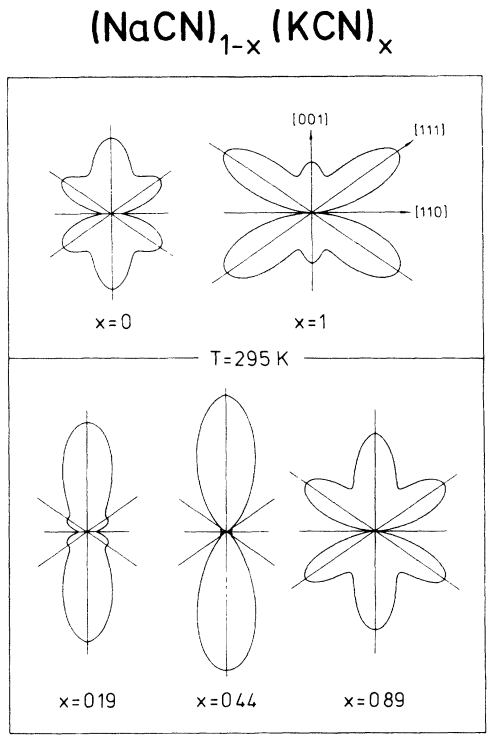

FIG. 11. Orientational probability of the CN^- molecules in the (110) plane as determined at 295 K for different concentrations x in $(NaCN)_{1-x}(KCN)_x$. The patterns for $x=0$ and 1 were calculated using the coefficients γ_4 and γ_6 given by Rowe *et al.* (Ref. 23) and Loidl *et al.* (Ref. 8).

error bars determined for $x=0.89$ and 1, $\gamma_6(x)$ has a clear minimum at an intermediate concentration. In contrast, $\gamma_4(x)$ exhibits a distinct maximum near $x=0.5$ and changes sign close to $x=1$. The data are in reasonable agreement with previous results for $x=0.02$ and 0.95 obtained from powder-diffraction experiments.[19] Previous results[19] for $x=0.19$ could not be verified. The concentration dependence of both coefficients is well described by $x(1-x)$, which is also the concentration dependence of random-strain fields in $(NaCN)_{1-x}(KCN)_x$. The solid lines in Fig. 10 are the fits to the data of this expression superimposed on a linear background of nonzero slope. We believe that Fig. 10 gives further evidence that $(NaCN)_{1-x}(KCN)_x$ is dominated by random strains.

The angular distributions of the CN^- molecule at room temperature derived from the expansion coefficients γ_4 and γ_6 are illustrated in Fig. 11. Results of the present work are compared to the angular distribution calculated earlier for $x=0$ and 1.[8,23] The maximum of the orientational probability along $\langle 100\rangle$ in $x=0$ increases when cationic disorder is introduced, while the relative maximum along $\langle 111\rangle$ decreases and vanishes for $x=0.44$. As x increases towards $x=0.89$, the probability along $\langle 100\rangle$ directions decreases again in favor of an increased probability for $\langle 111\rangle$ orientations. Finally, for $x=1$ the orientational distribution can be described by predominant $\langle 111\rangle$ orientations.[8,23] At $T=100$ K the analysis of the measured structure factors suggests a dominance of $\langle 100\rangle$ directions for $x=0.19$ and 0.44. However, due to an enhanced diffuse component, a correct structure-factor determination becomes more difficult at low temperatures. Therefore, the quantitative results are of low reliability and are not presented here.

Similar results were derived for mixed crystals of the related systems $(KBr)_{1-x}(KCN)_x$ and $(NaCl)_{1-x}(NaCN)_x$ by NMR techniques[25,26] and neutron experiments.[8] At low T the CN molecules were found to be predominantly oriented along $\langle 100\rangle$ directions, with minimum orientational probabilities along $\langle 111\rangle$. In the case of $(KBr)_{1-x}(KCN)_x$, the neutron results[8] for $x=0.53$ and NMR results[25] for $x=0.50$ are in reasonable agreement. However, substitutional discrepancies exist between these experiments and a molecular-dynamics simulation[27] which revealed preferential $\langle 111\rangle$ orientations of the CN^- molecules in $(KBr)_{1-x}(KCN)_x$. These discrepancies probably result from unrealistic conditions of the potential parameters used in the simulation. In general, the experimental results imply that both low T and strong substitutional disorder result in the predominance of $\langle 100\rangle$ CN^- orientations. This seems to be a universal feature of related cyanide mixed systems.

IV. SUMMARY

A detailed single-crystal neutron-diffraction study of $(NaCN)_{1-x}(KCN)_x$ has been performed for concentrations of $x=0.19$, 0.44, and 0.89. For all concentrations the line shapes deviate from the $A/q+B/q^2$ profile, predicted for crystals with elastic defects. (Due to the undiluted CN^- sublattice, the distance of neighboring elastic defects is $\sqrt{2}a/2$.) For $x=0.89$, diffuse contributions of almost exponential line shapes were found (Fig. 9), which exhibit a strong **Q** dependence in accordance with the theoretical predictions by Mayer and Cowley.[12,13] For $x\approx x_c$ a two-dimensional melting transition was proposed. Crystals with $x\lesssim x_c$ might be characterized by fluctuations which are frozen-in close to the planar instability.

The T dependence of the diffuse intensities are very different for the mixed crystals investigated (Figs. 2, 4, and 6). $(NaCN)_{0.81}(KCN)_{0.19}$ displays a diffuse contribution $I_{\rm diff}\sim 1/T^2$ at high temperatures, as predicted in a pure random-field model in the high-T limit. $(NaCN)_{0.56}(KCN)_{0.44}$ is a strong random-field system where the high-T approximation is already violated at room temperature; $I_{\rm diff}(T)$ increases much more weakly than $1/T^2$ for decreasing temperatures. Higher-order terms probably have to be taken into account in the expansion of $\tanh(h^2/T^2)$ for the random-strain concept[15,16] to be still applicable. $(NaCN)_{0.11}(KCN)_{0.89}$ transforms to a coexistence of cubic and rhombohedral phases at $T\approx 100$ K. $I_{\rm diff}\sim 1/T^2$ holds at high temperatures and exhibits a stronger T dependence for $T<150$ K.

At room temperature the orientational distribution of the CN^- molecules was determined by detailed structure-factor analysis. A strong concentration dependence was found for the reorientational behavior. We believe that the experimental evidence points to a domina-

tion of $(NaCN)_{1-x}(KCN)_x$ by random fields, with a tendency to pin the elastic defects along ⟨100⟩. At intermediate concentrations, random strains act as ⟨100⟩ defects and overcome the rotation-translation coupling. This strong random-strain–orientation coupling results in an almost single-ion behavior of the CN^- molecules, despite a fully occupied sublattice.

ACKNOWLEDGMENTS

This work has been funded by the German Federal Minister for Research and Technology [Bundesminister für Forschung und Technologie (BMFT)] under Contract No. 03-L01MAI-0(C1-56).

[1]F. Lüty, in *Defects in Insulating Crystals,* edited by V.M. Turkevich and K. K. Swartz (Springer-Verlag, Berlin, 1981), pp. 69–89.
[2]K. Knorr, Phys. Scr. **T19**, 531 (1987).
[3]A. Loidl, Annu. Rev. Phys. Chem. **40**, 29 (1989).
[4]J. M. Rowe, J. J. Rush, D. G. Hinks, and S. Susman, Phys. Rev. Lett. **43**, 1158 (1979).
[5]K. H. Michel and J. M. Rowe, Phys. Rev. B **22**, 1417 (1980).
[6]A. Loidl, M. Müllner, G. J. McIntyre, K. Knorr, and H. Jex, Solid State Commun. **54**, 367 (1985).
[7]K. Knorr and A. Loidl, Phys. Rev. Lett. **57**, 460 (1986).
[8]A. Loidl, K. Knorr, J. M. Rowe, and G. J. McIntyre, Phys. Rev. B **37**, 389 (1988).
[9]A. Loidl, T. Schräder, K. Knorr, R. Böhmer, B. Mertz, G. J. McIntyre, T. Vogt, H. Mutka, M. Müllner, H. Jex, and S. Haussühl, Z. Phys. B **75**, 81 (1989).
[10]P. Wochner, E. Burkel, J. Peisl, C. M. E. Zeyen, and W. Petry, in *Springer Proceedings in Physics* (Springer-Verlag, Berlin, 1989), Vol. 37, p. 280.
[11]P. Wochner, Ph.D. thesis, Universität München, 1988.
[12]A. P. Mayer and R. A. Cowley, J. Phys. C **21**, 4827 (1988).
[13]A. P. Mayer and R. A. Cowley, J. Phys. C **21**, 4835 (1988).
[14]T. Schräder, A. Loidl, and T. Vogt, Z. Phys. B (to be published).
[15]K. H. Michel, Phys. Rev. Lett. **57**, 2188 (1986); Phys. Rev. B **35**, 1404 (1987); **35**, 1414 (1987).
[16]K. H. Michel, Z. Phys. B **68**, 259 (1987); C. Bostoen and K. H. Michel, *ibid.* **71**, 369 (1988).
[17]J. Ortz Lopez, Ph.D. thesis, University of Utah, 1983; F. Lüty and J. Ortiz Lopez, Phys. Rev. Lett. **50**, 1289 (1983).
[18]A. Loidl, T. Schräder, R. Böhmer, K. Knorr, J. K. Kjems, and R. Born, Phys. Rev. B **34**, 1238 (1986).
[19]T. Schräder, A. Loidl, and T. Vogt, Phys. Rev. B **39**, 6186
[20]T. Schräder, A. Loidl, T. Vogt, and V. Frank, Physica B (Amsterdam) **156&157**, 195 (1989); T. Schräder, A. Loidl, M. Müller, and V. Frank, in *Springer Proceedings in Physics* (Springer-Verlag, Berlin, 1989), Vol. 37, p. 256.
[21]C. M. E. Zeyen, R. Chagnon, F. Disdier, and H. Morin, Rev. Phys. Appl. **19**, 789 (1984).
[22]R. S. Seymour and A. W. Pryor, Acta Crystallogr. Sect. B **26**, 1487 (1970).
[23]J. M. Rowe, D. G. Hinks, D. L. Price, S. Susman, and J. J. Rush, J. Chem. Phys. **58**, 2039 (1973).
[24]S. L. Altmann and A. P. Cracknell, Rev. Mod. Phys. **37**, 19 (1965).
[25]J. H. Walton and M. S. Conradi (unpublished).
[26]S. Elschner and J. Petersson, J. Phys. C **19**, 3373 (1986).
[27]L. J. Lewis and M. L. Klein, J. Phys. Chem. **91**, 4990 (1987).